

## How does extratropical warming affect ENSO?

Haijun Yang

Department of Atmospheric Science and Key Laboratory for Severe Storm and Flood Disasters, School of Physics, Peking University, Beijing, China

Qiong Zhang

State Key Laboratory of Numerical Modeling for Atmospheric Science and Geophysical Fluid Dynamics (LASG), Institute of Atmospheric Science, Chinese Academy of Sciences, Beijing, China

Yafang Zhong, Steve Vavrus, and Zhengyu Liu

Center for Climatic Research and Department of Atmospheric and Oceanic Sciences, University of Wisconsin-Madison, Madison, Wisconsin, USA

Received 28 September 2004; revised 1 November 2004; accepted 7 December 2004; published 11 January 2005.

[1] Idealized experiments in a coupled climate model show that the remote impact of the extratropics on the tropics can modulate the behavior of El Niño-Southern Oscillation (ENSO) phenomenon. An extratropical warming can weaken the Hadley cells and slow down the shallow meridional overturning circulations in the upper Pacific, causing reductions in the equatorward cold water supply and the equatorial upwelling and thus a weakened stratification of the equatorial thermocline. Therefore, weaker and longer ENSO cycle would occur in the stabilized equatorial coupled system resulted from the extratropical warming. **Citation:** Yang, H., Q. Zhang, Y. Zhong, S. Vavrus, and Z. Liu (2005), How does extratropical warming affect ENSO?, *Geophys. Res. Lett.*, 32, L01702, doi:10.1029/2004GL021624.

### 1. Introduction

[2] Paleoclimatic studies reveal that El Niño-Southern Oscillation (ENSO) has undergone significant climate shifts in the history [Cole, 2001; Liu *et al.*, 2000]. It has also changed during the past two decades [Fedorov and Philander, 2000]. These findings have led to speculations that ENSO may be subject to change in the future as a result of global warming. However, uncertainties and disputes about ENSO behavior in a warming climate exist for different models [Collins, 2000a]. Forced by a future greenhouse warming, ENSO amplitude could be increased due to a sharper equatorial thermocline [Timmermann *et al.*, 1999; Collins, 2000b], or decreased due to a reduced time-mean zonal sea surface temperature (SST) gradient [Knutson *et al.*, 1997], or even unchanged because of a negligible changes in mean temperature and zonal SST gradient in the equatorial Pacific [Tett, 1995; Meehl *et al.*, 1993]. ENSO frequency also could be increased due to the increase in meridional temperature gradients [Collins, 2000b] or unchanged [Knutson *et al.*, 1997]. The ENSO behavior appears to depend strongly on the mean climate, which in turn is determined by the model physics, resolution and sub-scale processes [Collins, 2000a].

[3] This study focuses on a nonlocal mechanism of the ENSO climate shift in a warmed climate. Although ENSO primarily originates in the tropics, studies have shown that

the extratropical climate change can significantly influence the tropics through both the atmospheric bridge of Hadley cells and oceanic tunnel of meridional overturning circulations [Wang and Weisberg, 1998; Weaver, 1999; Wang, 2002; Liu and Yang, 2003]. However, there is still lack of detailed discussions on the dynamical processes that are responsible for extratropical-originated ENSO climate change. Here, we reveal the crucial role of oceanic dynamic feedbacks in determining the ENSO behavior through idealized global warming experiments.

[4] The global climate model used is the Fast Ocean-Atmosphere Model (FOAM) [Jacob, 1997]. Its atmospheric component (R15) is a parallel version of the NCAR-CCM3 and its ocean component was developed following the GFDL-MOM with a resolution of  $1.4^\circ \times 2.8^\circ \times 32$  levels. Without flux adjustment, the control simulation (CTRL) has been integrated for over 1000 years, showing no climate drift. The simulated ENSO has a realistic amplitude and a period of 3–5 years [Liu *et al.*, 2000]. Experiments are performed to study the sensitivity of ENSO to extratropical climate warming. All the experiments start from the 800-th year of the CTRL and are integrated for 200 years, when the upper ocean has reached quasi-equilibrium. Specifically, to assess the full impact of the extratropical forcing on ENSO behavior, a “partial coupling” experiment (Atmosphere Bridge/Ocean Tunnel: ABOT) in which a homogenous  $2^\circ\text{C}$  SST warming is “seen” by both the atmosphere and ocean in the extratropics ( $>|30^\circ|$  latitude) and is then “carried” equatorward through both the atmospheric and oceanic bridges. The ocean and atmosphere in ABOT is fully coupled within the tropics ( $<|30^\circ|$  latitude), but partially coupled in the extratropics where the atmosphere is forced by mean seasonal cycle of heat flux from the CTRL plus a heat flux anomaly originated from the  $2^\circ\text{C}$  SST anomaly. Note that the  $2^\circ\text{C}$  SST forcing and the prescribed SST seasonal cycle are only applied to the regions without sea ice. There is still fully coupled between sea ice and atmosphere. In general, a warm SST in the extratropics forces a SST warming of about half its magnitude in the tropics, representing a significant control of the extratropical climate on tropical climate.

### 2. Changes in ENSO Variability

[5] The statistics of the ENSO variability show extensive changes in amplitude, frequency and spatial pattern. The

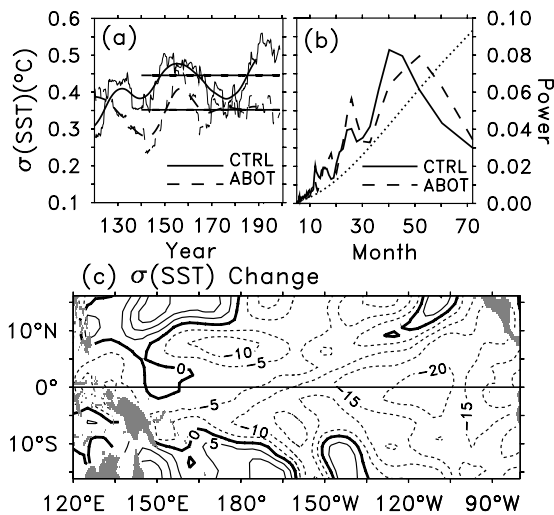


**Figure 1.** (a) Time series of the standard deviations (SD) of the monthly SST anomalies averaged over Nino-3 region ( $150^{\circ}\text{W}$ – $90^{\circ}\text{W}$ ,  $5^{\circ}\text{N}$ – $5^{\circ}\text{S}$ ), (b) Power spectrum of Nino-3 SST anomalies, and (c) Spatial pattern of the percentage change in the tropical SST SD. The SST anomalies are obtained by first removing the mean annual cycle of each run and then the secular linear trend of each run. A band-pass filter of 5–85 months is further applied to the SST anomalies to extract the ENSO signals. In (a) and (b), the solid lines are for the CTRL and the dashed lines for ABOT. In (a), only the last 80 years data are plotted for clearness; a low-pass filter with a sliding window of 10-year wide is used to calculate the SD that are plotted as the thin curves; the 21-year running mean is also plotted as the thick curves; the thick dashed straight lines represent the mean SD over the last 60 years. In (b), the primary peaks are located at the 40th and 50th month for CTRL and ABOT, respectively. Both peaks are well above the 95% confidence level denoted by the dotted line. In (c), the percentage change is calculated as the SD difference between ABOT and CTRL divided by that in CTRL in the last 60 years (unit in %).

time evolution of the Nino-3 SST shows a reduced amplitude (Figure 1). The mean standard deviation (SD) of the Nino-3 SST anomaly for the last 60 years is  $0.44^{\circ}\text{C}$  in CTRL and  $0.35^{\circ}\text{C}$  in ABOT, showing a 20% reduction in amplitude (Figure 1a). This reduction passes the F-test of 95% significance level. The power spectrum of Nino-3 SST (Figure 1b) has a primary peak located at the 40th month for CTRL and the 50th month for ABOT, respectively, showing a shift to longer period of the ENSO in response to the extratropical warming. This shift is statistically robust because it is also present in an arbitrary period of the time series that excludes the first 20 years, as well as in the raw data sets that have no filtering applied. The amplitude in the tropical interannual variability is not uniformly reduced. The largest decrease (more than 20%) occurs in the central and eastern tropical Pacific, while in the warm pool region the average decrease is 5% and is narrowly confined to within  $10^{\circ}$  of the equator (Figure 1c). Moreover, El Niño and La Niña, which consist of the positive and negative phases of the ENSO cycle, respectively, are not affected symmetrically in the warmer climate (figure not shown).

Statistically, compared with the La Niña, the El Niño is less suppressed by the extratropical warming. The simulation shows a skewed effect of the warming on the ENSO cycle, suggesting that warm events will happen more frequently than cold events in this warmer climate.

### 3. Changes in the Mean Climate

[6] The decrease in ENSO amplitude in the warmer climate is due to the relaxation of the equatorial trade winds, the weakened vertical temperature stratification and the deepening in the equatorial thermocline (Figure 2). These changes in the mean state play critical roles in determining the stability of the tropical ocean-atmosphere coupling modes [Fedorov and Philander, 2001]. The weakening in mean equatorial trade wind (Figure 2a) tends to reduce the east-west tilt of the equatorial thermocline and thus suppress the cold water upwelling in the eastern equatorial Pacific. The subsurface water warms more than the surface water (Figure 2b) (This is particularly clear in the eastern Pacific), resulting in a reduced vertical temperature gradient. The depth of the mean  $20^{\circ}\text{C}$  isotherm, a proxy of thermocline depth, is therefore moved downward by more than 20 meters in response to the thermocline warming. All these changes tend to stabilize the natural

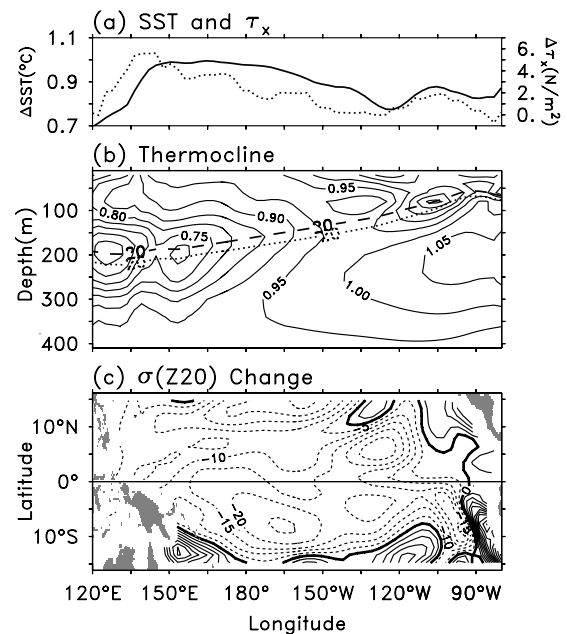


**Figure 2.** Mean climate changes in (a) SST (solid line) and zonal wind stress ( $\tau_x$ , dotted line) and (b) the thermocline temperature in ABOT, averaged in a  $5^{\circ}\text{N}$ – $5^{\circ}\text{S}$  equatorial strip of the Pacific. In (a), the scale for SST change ( $^{\circ}\text{C}$ ) is labeled at the left vertical coordinate and that for  $\tau_x$  change ( $10^{-3} \text{ N/m}^2$ ) is labeled at the right. The positive  $\tau_x$  anomaly implies that the equatorial trade winds are relaxed because the mean trade winds are negative (westward). In (b), the thick dashed and dotted lines represent the depth of the  $20^{\circ}\text{C}$  isotherm in CTRL and ABOT, respectively. (c) Spatial pattern of the SD percentage change in  $20^{\circ}\text{C}$  isotherm depth, which is calculated as the SD difference between ABOT and CTRL divided by that in CTRL in the last 60 years (unit in %).

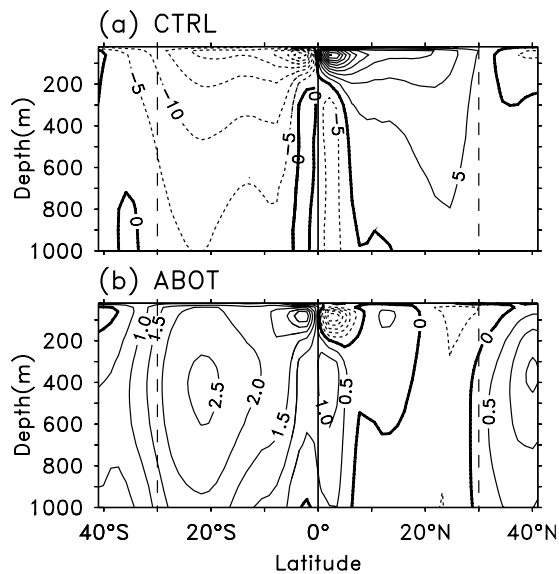


**Figure 3.** Shallow meridional overturning circulations in the upper Pacific for (a) the CTRL and (b) the change in ABOT averaged in the last 60 years. The latter shows a more than 10% reduction in the meridional overturning circulations in both hemispheres. The unit in (a) and (b) is Sv ( $1 \text{ Sv} = 10^6 \text{ m}^3/\text{s}$ ).

modes of oscillation of the tropical coupled ocean-atmosphere system, and eventually damp the ENSO variability [Fedorov and Philander, 2001; Timmermann, 2001]. Furthermore, the overall warming in the upper equatorial Pacific as well as the suppressed cold water upwelling cause the change in ENSO variability to be strongly skewed, with El Niño being affected less than La Niña.

[7] The changes in equatorial atmospheric trade winds and oceanic thermocline do not, however, originate locally within the tropics, but are remotely driven by changes in the extratropical climate. After the onset of the extratropical warming in ABOT, the Hadley cells in both hemispheres are weakened in response to the reduced meridional SST contrast. The weaker Hadley cells reduce the surface wind convergence towards the Intertropical Convergence Zone (ITCZ) and, in turn reduce the equatorial trade winds (Figure 2a) and the local upwelling [Liu and Yang, 2003]. In the ocean, the meridional overturning circulations slow down in response to the weakened Hadley cells (Figure 3b), resulting in a less equatorward cold water transport and a weaker equatorial upwelling. At the same time, the warm extratropical SST anomalies subduct equatorward by the mean circulation (Figure 3a). Both of these effects increase the temperature and depth of the equatorial thermocline, and weaken the vertical temperature gradient in the tropics (Figure 2b). By the way, the equatorial zonal SST contrast is enhanced by about  $0.2^\circ\text{C}$  (Figure 2a), suggesting that the “ocean dynamical thermostat” is valid in our complex coupled GCM, consistent with the studies in simplified coupled models [e.g., Clement *et al.*, 1996].

[8] The decrease in ENSO amplitude is consistent with the decrease in the equatorial warm water volume (WWV) variability (Figure 2c). Although the mean WWV, defined as the water above  $20^\circ\text{C}$  isotherm over the region  $5^\circ\text{S}$ – $5^\circ\text{N}$ ,

$120^\circ\text{E}$ – $80^\circ\text{W}$  [Meinen and McPhaden, 2000], expands downward as a result of the warmer equatorial thermocline (Figure 2b), the WWV variability is significantly reduced due to the weakening of the equatorial temperature stratification. The SD of  $20^\circ\text{C}$  isotherm depth is decreased by more than 15% in the equatorial region, with the change most visible in the eastern Pacific (Figure 2c) that is consistent with the larger SST change there. The WWV plays an important dynamical role in the oscillation of the ENSO cycle by controlling the temperature of waters upwelled in the eastern equatorial Pacific [Jin, 1997a, 1997b], which in turn controls the coupling between the thermocline and SST there. The decrease in ENSO frequency can be explained in terms of the meridional overturning circulation change. The slowdown of this meridional circulations retard a buildup (purge) of excess heat content along the equator, causing a shift in the frequency of WWV variability and thus a longer time scale for the ENSO cycle (Figure 1b). This is confirmed by another experiment in which the extratropical atmosphere is only forced by the mean seasonal cycle heat flux from the CTRL (Q. Zhang *et al.*, Anatomizing the extratropical modulation of ENSO, submitted to *Climate Dynamics*, 2004). There, the meridional overturning circulations remain unchanged, so do the frequencies of WWV and ENSO.

[9] The oceanic tunnel associated with the meridional overturning circulation change plays a more important role than the atmospheric bridge in the regulation of the ENSO behavior in a quasi-equilibrium system. The oceanic tunnel and the atmospheric bridge act on different time scales. The former occurs on interannual to decadal time scales, while the latter occurs on monthly time scales. Almost two-thirds of the mean SST warming is accomplished in the first several months, when the oceanic process has not yet taken effect. The ENSO amplitude is not reduced. Instead, it is enhanced slightly in the first 50 years of the simulation (figure not shown). This is consistent with the argument that the interannual variability may be increased because of a more energetic air-sea interaction in a warmer climate [e.g., Timmermann *et al.*, 1999]. However, the oceanic tunnel, while only contributing a small portion of the equatorial mean SST change, dominates more than 80% of the thermocline temperature change [Liu and Yang, 2003]. It is this slow oceanic process that reverses the effect of the atmospheric bridge, stabilizes the tropical coupled system and weakens the ENSO variability.

#### 4. Summaries and Discussions

[10] This study highlights a nonlocal mechanism in which ENSO behavior depends critically on the extratropical climate conditions, because the tropical mean state and thus the stability of the tropical coupled ocean-atmosphere system can be remotely determined by the extratropics. The oceanic tunnel that connects the extratropics to the tropics plays the most critical role. A weaker and longer ENSO cycle is likely in a future warmed climate. An extratropical climate warming could slow down both the Hadley cells and the meridional overturning circulations, resulting in reductions in the equatorward cold water supply and the equatorial upwelling, and thus a weakened stratification of the equatorial thermocline. These changes, together with the reduced equatorial trade wind associated with the weakened



Hadley cells, can stabilize the equatorial coupled system and cause weaker ENSO variabilities.

[11] This nonlocal mechanism of ENSO change should also work in a climate forced by an anomalous cooling. This is consolidated by a global “cooling” experiment of the FOAM in which the solar constant is suddenly reduced by  $8 \text{ W/m}^2$ . This experiment is integrated for 130 years and the last 50 years data are analyzed. The quasi-equilibrium response of the Pacific SST shows three SST cooling maxima located at  $35^\circ\text{--}60^\circ$  in both hemispheres ( $-0.9^\circ\text{C}$  for the North Hemisphere and  $-1.2^\circ\text{C}$  for the South Hemisphere) and the central-east equatorial Pacific ( $-0.6^\circ\text{C}$ ), respectively. This SST pattern is nearly antisymmetric to that in the partial coupling experiment of ABOT. The ENSO amplitude is increased by as much as 28% in the tropical coupled system destabilized by the increased cold water supply from the extratropics due to enhanced Hadley cells and meridional overturning circulations.

[12] The extratropical modulation on ENSO behavior is also justified by the observation studies that the ENSO regime shift in the 1970s is closely linked to the regime shift in the North Pacific decadal oscillation [e.g., Zhang *et al.*, 1998], and a recent simplified coupled model study by Sun *et al.* [2004], who identified an increase in ENSO amplitude by an enhanced subtropical cooling. The stronger subtropical cooling reduces the temperature of the water feeding the equatorial undercurrent through the oceanic tunnel. The resulting colder equatorial upwelling water tends to increase the equatorial zonal SST contrast. The ENSO strengthens in response to this destabilizing forcing. Note that the atmospheric component in Sun *et al.* [2004] includes only the zonal wind simply coupled to the zonal SST gradient. As a result, the Bjerknes positive feedback works very well. This is different from our model in which the tropical wind is nonlocally determined by the Hadley cells.

[13] Our primary results show a milder ENSO is likely in a warmer climate. The results could be model dependent because different GCM simulations show different ENSO responses to the mean climate change and the sensitivity of ENSO to any kind of changes depends strongly on the criticality of ENSO [Collins, 2000a; Timmermann, 2001]. However, this study provides one possible mechanism for ENSO climate shift which could help to better understand the evolution of ENSO in the past as well as in the present and future.

[14] **Acknowledgments.** This work is jointly supported by NOAA, NASA and DOE of the United States and the NSF of China (No.40306002 40333030), the Chinese Academy of Sciences Project ZKCX2-SW-210, the Foundation for Open Projects of the Key Lab of Physical Oceanography, Ministry of Education of China (No. 200303) and the National Basic Research Program of China (No. 2004CB720208). The authors thank Erin Hokanson and Pat Behling at CCR in Univ. Wisconsin-Madison for data processing and English checking. Center for Climatic Research contribution number 865.

## References

- Clement, A. C., R. Seager, M. A. Cane, and S. E. Zebiak (1996), An ocean dynamic thermostat, *J. Clim.*, *9*, 2190–2196.
- Cole, J. (2001), A slow dance for El Niño, *Science*, *291*, 1496–1497.
- Collins, M. (2000a), Understanding uncertainties in the response of ENSO to greenhouse warming, *Geophys. Res. Lett.*, *27*, 3509–3513.
- Collins, M. (2000b), The El-Niño Southern Oscillation in the second Hadley Centre coupled model and its response to greenhouse warming, *J. Clim.*, *13*, 1299–1312.
- Fedorov, A. V., and S. G. Philander (2000), Is El Niño changing?, *Science*, *288*, 1997–2002.
- Fedorov, A. V., and S. G. Philander (2001), A stability analysis of Tropical ocean-atmosphere interaction: Bridging measurements and theory for El Niño, *J. Clim.*, *14*, 3086–3101.
- Jacob, R. (1997), Low frequency variability in a simulated atmosphere ocean system, Ph.D. thesis, 155 pp., Univ. of Wis., Madison.
- Jin, F.-F. (1997a), An equatorial ocean recharge paradigm for ENSO. Part I: Conceptual model, *J. Atmos. Sci.*, *54*, 811–829.
- Jin, F.-F. (1997b), An equatorial ocean recharge paradigm for ENSO. Part II: A stripped-down coupled model, *J. Atmos. Sci.*, *54*, 830–847.
- Knutson, T. R., S. Manabe, and D. Gu (1997), Simulated ENSO in a global coupled ocean model: Multidecadal amplitude modulation and  $\text{CO}_2$  sensitivity, *J. Clim.*, *10*, 138–161.
- Liu, Z., and H. Yang (2003), Extratropical control of tropical climate, the atmospheric bridge and oceanic tunnel, *Geophys. Res. Lett.*, *30*(5), 1230, doi:10.1029/2002GL016492.
- Liu, Z., J. Kutzbach, and L. Wu (2000), Modeling climate shift of El Niño variability in the Holocene, *Geophys. Res. Lett.*, *27*, 2265–2268.
- Meehl, G. A., G. W. Branstator, and W. M. Washington (1993), Tropical Pacific interannual variability and  $\text{CO}_2$  climate change, *J. Clim.*, *6*, 42–63.
- Meinen, C. S., and M. J. McPhaden (2000), Observations of warm water volume changes in the equatorial Pacific and their relationship to El Niño and La Niña, *J. Clim.*, *13*, 3551–3559.
- Sun, D.-Z., T. Zhang, and S.-I. Shin (2004), The effect of subtropical cooling on the amplitude of ENSO: A numerical study, *J. Clim.*, *17*, 3786–3798.
- Tett, S. (1995), Simulations of El Niño–Southern Oscillation-like variability in a global AOGCM and its response to  $\text{CO}_2$  increase, *J. Clim.*, *8*, 1473–1502.
- Timmermann, A. (2001), Changes of ENSO stability due to greenhouse warming, *Geophys. Res. Lett.*, *28*, 2061–2064.
- Timmermann, A., M. Latif, A. Bacher, J. Oberhuber, and E. Roeckner (1999), Increased El Niño frequency in a climate model forced by future greenhouse warming, *Nature*, *398*, 694–696.
- Wang, C. (2002), Atmospheric circulation cells associated with the El Niño–Southern Oscillation, *J. Clim.*, *15*, 399–419.
- Wang, C., and R. H. Weisberg (1998), Climate variability of the coupled tropical-extratropical ocean-atmosphere system, *Geophys. Res. Lett.*, *25*, 3979–3982.
- Weaver, A. J. (1999), Extratropical subduction and decadal modulation of El Niño, *Geophys. Res. Lett.*, *26*, 743–746.
- Zhang, R. H., L. M. Rothstein, and A. J. Busalacchi (1998), Origin of warming and El Niño change on decadal scales in the tropical Pacific Ocean, *Nature*, *391*, 879–883.

Z. Liu, S. Vavrus, and Y. Zhong, Center for Climatic Research and Department of Atmospheric and Oceanic Sciences, University of Wisconsin-Madison, Madison, WI 53706–1695, USA.

H. Yang, Department of Atmospheric Science and Key Laboratory for Severe Storm and Flood Disasters, School of Physics, Peking University, 209 Chengfu Road, Beijing, China 100871. (hjiang@pku.edu.cn)

Q. Zhang, State Key Laboratory of Numerical Modeling for Atmospheric Science and Geophysical Fluid Dynamics (LASG), Institute of Atmospheric Science, Chinese Academy of Sciences, Beijing, China 100029.